

## Fragments with $6 \leq Z \leq 15$ Emitted from Au Bombarded with 2.1-GeV/Nucleon $^{16}\text{O}$ Ions and 2.1-GeV Protons\*

James D. Sullivan, P. B. Price,† and H. J. Crawford  
*Department of Physics, University of California, Berkeley 94720*

and

Marian Whitehead  
*California State University, Hayward, California 94542*  
 (Received 30 November 1972)

In the reaction  $34\text{-GeV } ^{16}\text{O} + \text{Au} \rightarrow Z$ , fragments with  $6 \leq Z \leq 15$  are emitted with higher than geometric cross section and with a broad distribution of energies extending down to  $\sim 0.8$  MeV/nucleon. Such low kinetic energies are far below the hard-sphere Coulomb barrier and may imply extreme distortions of a nucleus raised to high temperature by the  $^{16}\text{O}$  ion.

Using Lexan track detectors,<sup>1</sup> we have compared the energy spectra and charge spectra of low-energy fragments from a Au target bombarded with 2.1-GeV/nucleon  $^{16}\text{O}$  ions and with 2.1-GeV protons at the Bevatron. In the  $^{16}\text{O}$  interactions the yield of fragments with  $6 \leq Z \leq 15$  and  $1 \leq E \leq 5$  MeV/nucleon is an order of magnitude higher, their charges and kinetic energies tend to be lower, and their energy distribution is broader than in the proton interactions.

Figure 1 shows the geometry of the detector, which consists of two cones and a cylinder of 250- $\mu\text{m}$  Lexan polycarbonate surrounding an unbacked 7.4-mg/cm<sup>2</sup> Au target. Tracks of fragments originating in the Au and impinging on the plastic can be studied as a function of angle to the beam, from  $\sim 5^\circ$  to  $\sim 60^\circ$  and from  $\sim 120^\circ$  to  $\sim 175^\circ$ . Because of self-absorption in the target, we did not attempt to study tracks at angles of  $60^\circ$  to  $120^\circ$ . Following a three-stage process consisting of initial chemical etch plus intense ultra-

violet irradiation plus final chemical etch,<sup>2</sup> we measure two parameters for each fragment that can be related to its charge and energy: The length of the conical pit produced in the initial etch gives the etch rate, which is a measure of ionization rate; the length of the narrow tail produced in the final etch gives the range of the particle. Separate calibrations with low-energy beams of heavy ions permit range-etch-rate measurements to be converted to charge and energy. Particles with energies down to  $\sim 0.8$  MeV/nucleon can be identified in the interval  $6 \leq Z \leq 15$ , and rough estimates of charge can be made for particles with energies down to  $\sim 0.2$  MeV/nucleon. Our detector has a practical cutoff at low etch rate: At  $\sim 1$  MeV/nucleon it is difficult to detect fragments with  $Z < 6$ ; at  $\sim 5$  MeV/nucleon the minimum detectable charge moves up to  $\sim 8$ . (By modifying the etching conditions it is possible to optimize the detector for lighter or heavier fragments.)

The assembly was irradiated in the external beam line in an 8-in.-diam target chamber evacuated to  $\sim 10$  Torr. With the assistance of H. H. Heckman, D. Greiner, F. Bieser, and P. J. Lindstrom, the  $^{16}\text{O}$  beam was monitored continuously with a fast plastic scintillation counter  $\sim 1$  m downstream from the target chamber; the counter calibration was checked from time to time by exposing 100- $\mu\text{m}$  Ilford G5 emulsions to one or two beam pulses. The proton beam was monitored both with a secondary emission counter and radiochemically using  $^7\text{Be}$  activation of a polyethylene target. The beam fluences were  $(1.7 \pm 0.3) \times 10^{10}$  for  $^{16}\text{O}$  and  $(2.08 \pm 0.1) \times 10^{12}$  for protons.

In both the  $^{16}\text{O}$  and proton irradiations, the angular distribution summed over all energies and

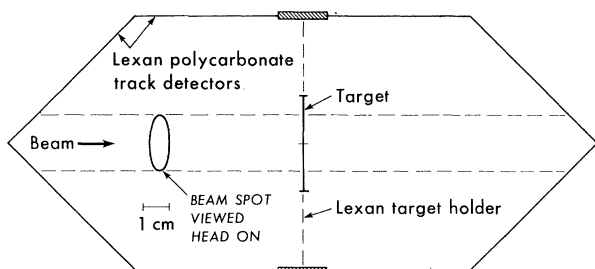


FIG. 1. Schematic diagram of the detector assembly. A free foil of Au target 7.4 mg/cm<sup>2</sup> thick was suspended in a cylindrically symmetric assembly of 250- $\mu\text{m}$ -thick Lexan polycarbonate track detectors and placed in a vacuum of  $\sim 10$  Torr.

over charges  $6 \leq Z \leq 15$  smoothly increases from the backward to the forward direction. The ratio of yields at  $45^\circ$  and at  $135^\circ$  is  $\sim 1.75$  for the  $^{16}\text{O}$  irradiation and  $\sim 2.0$  for the proton irradiation. The latter agrees with the ratio measured by Poskanzer, Butler, and Hyde (PBH)<sup>3</sup> for fragments with  $Z \sim 6$  emitted in a 5.5-GeV proton bombardment of a U target. Assuming an isotropic distribution in a center-of-momentum frame, we infer mean components of velocity of  $\sim 0.006c$  to  $0.008c$  in the forward direction for each irradiation.

The angular distribution of the more energetic fragments ( $E \sim 4$  MeV/nucleon) is more strongly forward peaked than that for all fragments, but is still a monotonic function of angle. We find no evidence in either the  $^{16}\text{O}$  or proton bombardment for preferential emission at a Mach angle such as would be expected if hydromagnetic waves were being excited in target nuclei.<sup>4</sup>

In Figure 2 we compare etch rate versus range distributions of  $\sim 300$  fragments emitted at  $45^\circ$  to the beam in (a) the  $^{16}\text{O}$  bombardment and (b) the proton bombardment. The same Au target was used in both exposures. Lexan strips from the two exposures were processed simultaneously and analyzed in parallel. Fission fragment tracks, which could easily be recognized because of their high etch rate and short range, were excluded from the sample of 300 tracks. The energy and charge of each fragment can be estimated by referring to the curves in Fig. 2. Individual elements are not clearly resolved, presumably because of the broad distribution of isotopes emitted. The data are not corrected for the finite target thickness, which would shift the distributions toward higher energy by as much as  $\sim 0.7$  MeV/nucleon.

The two distributions differ distinctly. One can see from the figure that the 300 fragments emitted in the  $^{16}\text{O}$  bombardment tend to have lower energy and lower charge than those emitted in the proton bombardment. When we break up the data into energy distributions for the individual charges, we find that for each charge (1) the most probable energy is lower, (2) the distribution is broader, and (3) the minimum energy is lower for the  $^{16}\text{O}$  bombardment than for the proton bombardment.

At energies above  $\sim 3$  MeV/nucleon our proton data are consistent with those of PBH.<sup>3</sup> Because of the finite thickness of their  $\Delta E$  detector, they were not able to observe particles of lower energy and they would therefore have missed most of

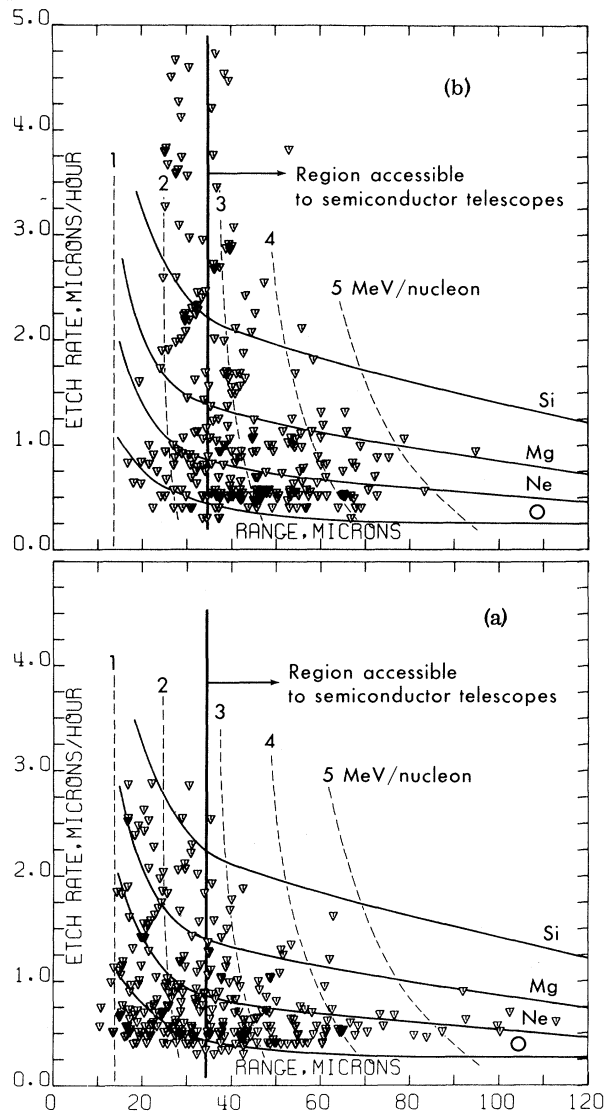


FIG. 2. Track etching rate versus particle range for fragments at  $45^\circ$  to the beam from (a)  $^{16}\text{O} + \text{Au}$  and (b)  $p + \text{Au}$ . Fission fragments have been excluded. The charge grid is based on a semiempirical fit to calibrations with beams of low-energy  $^{16}\text{O}$ ,  $^{28}\text{Si}$ ,  $^{40}\text{Ar}$ , and  $^{56}\text{Fe}$  ions. The vertical line shows the region accessible to semiconductor particle identifiers.

the events recorded in our  $^{16}\text{O}$  bombardment.

The cross section for producing the sum of all fragments in Fig. 2 is about 12 times higher in the  $^{16}\text{O}$  bombardment than in the proton bombardment. The cross section for the proton bombardment, when corrected for our cutoff at low etch rate, is consistent with that measured by PBH<sup>3</sup> for the same charges. When integrated over all angles, the cross section for the  $^{16}\text{O}$  bombardment is higher than the geometric cross section

for  $^{16}\text{O} + \text{Au}$  and implies multiple fragment emission. For  $Z \sim 8$ , the ratio  $\sigma(^{16}\text{O})/\sigma(p) \approx 25$ . With increasing  $Z$  the ratio decreases, as can be seen qualitatively in Fig. 2. For  $Z \geq 12$ ,  $\sigma(^{16}\text{O})/\sigma(p) \approx 3$ . In a separate scan for fission fragments, we measured  $\sigma(^{16}\text{O})/\sigma(p) \approx 3$ , consistent with the value of Katcoff and Hudis.<sup>5</sup> The calculated ratio of geometric cross sections is also  $\sim 2$ .

The most striking features of our  $^{16}\text{O}$ -induced disintegrations are the low kinetic energies of the fragments and the high cross sections for their production, which are not understood in terms of existing models of high-energy interactions.

In previous studies of proton-induced fragmentation of heavy nuclei, attempts have been made to fit the energy distributions to an evaporation model, but it has been necessary to include several adjustable parameters to reproduce the position and breadth of the peak and the shape of the high-energy tail. To match their most probable energies, PBH<sup>3</sup> required an effective Coulomb barrier,  $E_{\text{eff}}$ , which was about  $\frac{1}{2}$  the value calculated for a spherical fragment emitted from a spherical nucleus.

Deficiencies of the evaporation model are more severe when it is applied to our  $^{16}\text{O}$  data.  $E_{\text{eff}}$  must be reduced to less than  $\frac{1}{3}$  the hard-sphere value, and the smearing of the peaks is much more extreme than with the proton data.

We can perhaps understand qualitatively the very low Coulomb barrier if the disintegrating nucleus is extremely deformed, so that at scission the ejected fragment is far from the center of the residual nucleus. If the Au disintegrates into several fragments, their kinetic energies are lowered both because of the reduced Coulomb barrier and because of recoil.

We interpret our results as evidence that heavy ions can deposit more energy in a nucleus than can protons, resulting in higher nuclear temper-

atures. Considered as a liquid drop, the nucleus has a surface tension that decreases with increasing temperatures and may vanish at a critical point in the vicinity of the Fermi temperature.<sup>6</sup> With reduced surface tension, the fissility increases and multiple fragment emission at low kinetic energies becomes possible.

Until heavy-ion beam intensities can be increased by about a factor of  $10^3$  and other particle identifiers can be developed with much thinner  $\Delta E$  detectors, the present technique with plastic detectors appears to be unique. With a sandwich geometry we plan to look for direct evidence of multiple fragment emission by a single nucleus.

We thank the Bevatron operations staff under H. A. Grunder and W. D. Hartsough, and F. Lothrop for giving us their unlimited support and effort during the experiment. We also thank H. H. Heckman, D. Greiner, F. Bieser, and P. J. Lindstrom for their generous cooperation and extensive aid. We thank A. Smith for the activation analysis of the polyethylene. We appreciate the effort of N. Peery who made the large number of track measurements. We enjoyed useful conversations with A. M. Poskanzer, L. G. Moretto, and W. J. Swiatecki.

\*Work supported by the U. S. Atomic Energy Commission under Contract No. AT(04-3)-34.

†Miller Institute Professor, 1972-1973.

<sup>1</sup>P. B. Price and R. L. Fleischer, *Annu. Rev. Nucl. Sci.* **21**, 295 (1971).

<sup>2</sup>R. A. Stern and P. B. Price, *Nature (London)* **240**, 82 (1972).

<sup>3</sup>A. M. Poskanzer, G. W. Butler, and E. K. Hyde, *Phys. Rev. C* **3**, 882 (1971).

<sup>4</sup>A. E. Glassgold, W. Heckrotte, and K. M. Watson, *Ann. Phys. (New York)* **6**, 1 (1959).

<sup>5</sup>S. Katcoff and J. Hudis, *Phys. Rev. Lett.* **28**, 1066 (1972).

<sup>6</sup>W. A. Kuepper, unpublished.